

## Repositório ISCTE-IUL

---

Deposited in *Repositório ISCTE-IUL*:

2025-01-24

Deposited version:

Accepted Version

Peer-review status of attached file:

Peer-reviewed

Citation for published item:

Vaquero, Á. F., Teixeira, J., Matos, S. A., Arrebola, M., Costa, J. R., João M. Felício...Fonseca, N. J. G. (2023). Design of low-profile transmitarray antennas with wide mechanical beam steering at millimeter waves. *IEEE Transactions on Antennas and Propagation*. 71 (4), 3713-3718

Further information on publisher's website:

10.1109/TAP.2023.3243796

Publisher's copyright statement:

This is the peer reviewed version of the following article: Vaquero, Á. F., Teixeira, J., Matos, S. A., Arrebola, M., Costa, J. R., João M. Felício...Fonseca, N. J. G. (2023). Design of low-profile transmitarray antennas with wide mechanical beam steering at millimeter waves. *IEEE Transactions on Antennas and Propagation*. 71 (4), 3713-3718, which has been published in final form at <https://dx.doi.org/10.1109/TAP.2023.3243796>. This article may be used for non-commercial purposes in accordance with the Publisher's Terms and Conditions for self-archiving.

---

### Use policy

Creative Commons CC BY 4.0

The full-text may be used and/or reproduced, and given to third parties in any format or medium, without prior permission or charge, for personal research or study, educational, or not-for-profit purposes provided that:

- a full bibliographic reference is made to the original source
- a link is made to the metadata record in the Repository
- the full-text is not changed in any way

The full-text must not be sold in any format or medium without the formal permission of the copyright holders.

---

# Design of Low Profile Transmitarray Antennas with Wide Mechanical Beam Steering at Millimeter-Waves

Álvaro F. Vaquero, *Member, IEEE*, Jorge Teixeira, Sérgio A. Matos, *Senior Member, IEEE*, Manuel Arrebola, *Senior Member, IEEE*, Jorge R. Costa, *Senior Member, IEEE*, João M. Felício, *Member, IEEE*, Carlos A. Fernandes, *Senior Member, IEEE*, and Nelson J. G. Fonseca, *Senior Member, IEEE*

**Abstract**— Mechanical beam steering using a single Transmitarray (TA) can be a cost-effective solution for a high-gain antenna with wide-angle scanning. Elevation scanning can be achieved by a linear displacement of the feed parallel to the aperture. When designing compact terminals ( $F/D < 0.5$ ) with high gain ( $>20$  dBi) the aberrations caused by this mechanical movement become the main limiting factor for the maximum scanning range. This work presents a novel design method for devising the TA phase correction with an even distribution of these aberrations among all beam directions. A significant improvement in the scanning performance is achieved when compared with the conventional single-focus phase correction approach. To validate the proposed approach, we consider a TA design with  $F=50$  mm, in-plane dimension  $195 \times 145$  mm ( $F/D \cong 0.34$ ) operating at Ka-band (30 GHz). A multifocal TA design was manufactured using 3D printed unit-cells. To highlight the proposed concept, the antenna configuration is stripped to the bare minimum: a perforated dielectric slab with in-plane mechanical movements placed in front of a standard waveguide (WR28). This antenna scans up to  $50^\circ$ , with a gain of 25 dBi at 30 GHz, 2.5 dB of scan loss, SLL  $< -10$  dB and 1 dB-bandwidth of 6.7% (29 to 31 GHz).

**Index Terms**— Dielectric lens, Low focal distance Mechanical Beam Steering, Ka-band, Transmitarray, 3D printing, 5G Mobile Communications

## I. INTRODUCTION

With the continuous exploration of millimeter waves, fomented by next generation of mobile satellite communications, low-cost compact beam scanning antenna solutions assume a central role in this area of research. Several solutions have been proposed in the literature, such as the popular phased-array antennas [1], reconfigurable reflectarray or transmit-array antennas [2], [3], as low-profile solutions for electronic beam scanning. The main drawback of these solutions are their high cost, high losses, and power consumption, as well as the complexity in the design of the phase control of each element. To overcome these issues, passive reflectarray antennas have been also proposed for beam scanning applications. Like reflector-based solutions [4], a reflectarray commonly achieves beam scanning by

This work was supported in part by MCIN/AEI/10.13039/501100011033 within the project PID2020-114172RB-C21, by Gobierno del Principado de Asturias within project AYUD/2021/51706, and in part by FCT and under FEDER—PT2020 partnership agreement Project PTDC/EEL-TEL/30323/2017 - LISBOA-01-0145-FEDER-030323 and UIDB/50008/2020.

Á. F. Vaquero, and M. Arrebola are with the Department of Electrical Engineering, Universidad de Oviedo, Gijón, 33203, Spain (e-mail: fernandezvalvaro@uniovi.es; arrebola@uniovi.es).

J. Teixeira, Sérgio A. Matos and Jorge R. Costa are with the Instituto de Telecomunicações, Instituto Superior Técnico, Universidade de Lisboa, 1049-001 Lisbon, Portugal, and also with the Departamento de Ciências e Tecnologias da Informação, Instituto Universitário de Lisboa (Iscte-IUL),

displacing the feed from the focus through a spatial feeding mechanism [5], [6]. To obtain a good tradeoff between the spillover and the illumination tapering, the focal distance is comparable to the array aperture ( $F \cong D$ ). Thus, for large-scale reflectarray, the focal distance rapidly increases the profile of the antenna. Another alternative is based on quasi-optical beamformers [7], which provide interesting characteristics, such as wideband response and wide scanning range at the cost of bulky structures. For instance, the Luneburg lens provides an aberration-free scanning over an extended range but with  $F/D \sim 1$  [8]. In [9], a half-Luneburg lens demonstrates acceptable scanning performance while reducing the height by a factor of two ( $F/D \sim 0.5$ ). However, there is still a need to achieve further length reduction ( $F/D < 0.4$ ) to consider quasi-optical systems as a realistic alternative to phased-array antennas in applications that require low-profile designs.

In this context, TA antennas present some advantages over the aforementioned solutions: low-cost relative to phased-array or beamformers, more compact than reflector-based solutions, and they can reduce the  $F/D$  of a reflectarray, and additionally, the feed blockage is avoided. However, other limitations need to be tackled, such as multiband operation [10] and the antenna height [11]. In [11], a TA with an offset Fresnel phase correction was designed for wide beam scanning through only in-plane mechanical movements. The focal length used in this work is a compromise between the antenna height and scanning aberrations. Further reducing the focal length requires finding a new phase correction for the TA that can better cope with the beam distortions caused by the feed displacement. The recent approaches proposed for multifocal lenses for wide beam scanning [12]-[14] cannot be applied directly to TA due to the intrinsic flat geometry of the aperture. Some published works have proposed the use of either bifocal or parabolic phase corrections [15]-[17], or quadrfocal phase distributions [18]. In [15], a bifocal design was introduced by means of two TAs. In [16], a bifocal TA phase correction was defined by a weight average of two unifocal phase corrections, creating two pseudo-foci instead of well-defined focal positions. In [17], a parabolic ansatz for the TA phase distribution was used for minimizing the phase error for 4-beam multibeam antenna. In

1649-026 Lisbon, Portugal (e-mail: sergio.matos@iscte.pt; Jorge.Costa@iscte.pt).

João M. Felício is with the Centro de Investigação Naval (CINAV), Escola Naval, Instituto Universitário Militar (IUM), 2810-001 Almada, Portugal, and also with the Instituto de Telecomunicações, Instituto Superior Técnico, Universidade de Lisboa, 1049-001 Lisbon, Portugal (e-mail: joao.felicio@lx.it.pt).

Carlos A. Fernandes is with the Instituto de Telecomunicações, Instituto Superior Técnico, Universidade de Lisboa, 1049-001 Lisbon, Portugal (e-mail: carlos.fernandes@lx.it.pt).

Nelson J. G. Fonseca is with the European Space Agency, Antenna and Sub-Millimetre Waves Section, Noordwijk, The Netherlands. (e-mail nelson.fonseca@esa.int).

[18], a quadrifocal phase distribution was introduced to achieve a wide beam scanning considering that the source moves along the lens focal arch and for high  $F/D$  ratio ( $F/D = 1$ ). As far as the authors are aware, there is still lacking a general approach for designing TA antennas combining wide beam scanning and low focal distance ( $F/D < 0.4$ ). Existing approaches rely on blind optimization processes conditioned by the considering ansatz (bifocal, quadrifocal, parabolic) and though only for a specific design.

In this work, we propose a general method to address the design with low  $F/D$  and wide beam scanning performance. In summary, the method consists of constructing the TA phase correction iteratively by gradually perturbing the solution by adding new pseudo-foci, which provides a global minimization of the phase errors accounting for multiple source positions. The iterative nature of the method allows that the phase correction follows the natural scanning tendency of the considered solution, which cannot be known *a priori*. In addition to the obvious advantage of reducing the antenna height, working with a lower focal distance implies that the primary source can have lower gain, which further reduces the antenna complexity. The corresponding mechanical scanning approach is shown in Figure 1, obtaining that the  $360^\circ$  azimuth scanning is reached by rotating the complete antenna system. For a better comparison with the more conventional approach used in [11], the proposed method is validated through the design of a TA with the same aperture ( $195 \times 145 \text{ mm}^2$ ) and scanning range ( $\pm 50^\circ$ ) but with half of the focal length. The unit cell is a broadband solution based on a hollow square prism of polylactic acid (PLA) ( $\epsilon_r = 2.98$  and  $\tan \delta = 0.0148$  [19]) compatible with 3D printing. We confirm through full-wave simulations [20] that the improvements predicted by combined Geometric Optics and Physic Optics (GO-PO) analysis is effective, and a prototype is manufactured. The resulting antenna is composed of a perforated dielectric slab of PLA fed by an open-ended waveguide (WR28) placed at  $47.5 \text{ mm}$  ( $F/D = 0.34$ ). This antenna presents a very good scanning performance considering the low  $F/D$  value. For the nominal design frequency, the prototype has a 25 dBi gain with a scan loss of 1.5 dB when scanning up to  $50^\circ$  while preserving the SLL below  $-10 \text{ dB}$  for all the feed positions. Moreover, the broadband nature of the selected unit cells allows to demonstrate that the design method is still effective for a large bandwidth, from 29 to 31 GHz.

## II. MULTI-FOCAL APPROACH FOR TRANSMIT-ARRAY DESIGN

Ideal collimation is achieved when the phase distribution of the outgoing fields on the aperture is given by

$$g_{ap}^\alpha = \phi_{lens} + \phi_{in}^{x_s} = -k_0 \sin \alpha x \quad (1)$$

where  $x_s \in [x_{min}, x_{max}]$  is an arbitrary position of the source along the  $x$  direction and  $\alpha$  is the corresponding beam offset (Figure 1). In the context of a single flat passive aperture and impinging spherical wave front, perfect collimation in  $\alpha_0$  angular direction can only be exact for a single source position ( $x_s = x_0$ ), the lens focus  $P = (x_0, 0, -F)$ . In this case it follows from (1) the conventional unifocal Fresnel correction (as in [11])

$$\phi_{lens}^{x_0} = k_0 \sqrt{(x - x_0)^2 + y^2 + F^2} - k_0 \sin \alpha_0 x \quad (2)$$

The linear term of the phase error caused by the displacement of the feed relative to the focus position provides beam steering capability, however, it is limited by the aberrations that build up with this displacement [11]. These aberrations rapidly become the limiting factor for achieving wide beam scanning when low  $F/D$  ratios are considered. In Figure 2, using GO-PO analysis, we show how the design (1) performs for a  $F/D = 0.34$  ( $D = 145 \text{ mm}$ ). The aperture

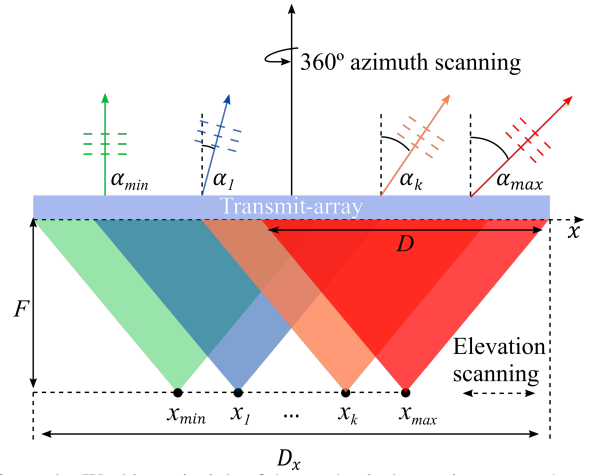


Figure 1 – Working principle of the mechanical scanning approach.

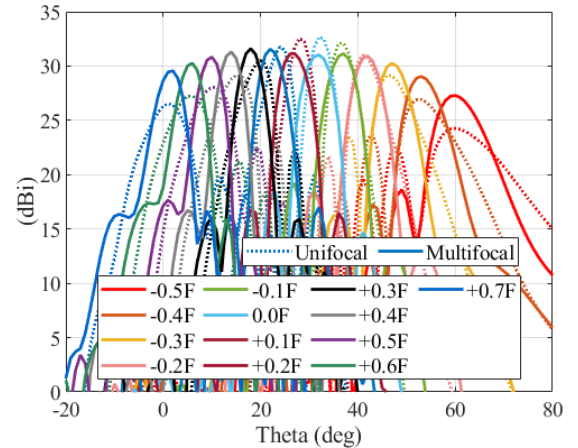


Figure 2– Comparison between simulated results with GO-PO of the performance of the unifocal and multifocal TA, with  $\alpha_0 = 32.5^\circ$ ,  $\sigma = 44.8 \text{ mm}$ , corresponding to  $\tau_{dB} = 10 \text{ dB}$ . Each curve corresponds to a different feed displacement along  $x_s$ .  $F/D = 0.34$ ,  $D = 145 \text{ mm}$ .

size is  $145 \times 195 \text{ mm}^2$ , the values that will be considered for our multifocal design example. As expected, the maximum gain (32.7 dBi) is obtained for the prescribed beam offset  $\alpha_0 = 32.5^\circ$  when the feed is placed at the lens focus. Note that  $\alpha_0$  is selected according to [11] to fairly compare both results.

The aberrations caused by the feed displacement greatly limit the scanning performance of the antenna. The 3 dB scanning range window is now  $[-15^\circ, 46^\circ]$  with high SLL (up to  $-5.6 \text{ dB}$ ) and the scan loss to achieve boresight is 6 dB. Clearly aberrations are the main cause for the gain reduction, overshadowing the natural scan loss of planar apertures given by projected aperture factor  $\cos \alpha$ , that for  $32^\circ$  to  $46^\circ$  scanning would only correspond to a 0.9 dB gain drop. This case contrasts with the unifocal design presented in [11], where a larger focal distance was considered,  $F/D = 0.7$ , which provides a 3 dB scanning range of  $[0^\circ, 50^\circ]$  with SLL below  $-10 \text{ dB}$ .

A first approach to circumvent this problem is to define the lens phase correction as a weighted average  $K$  unifocal corrections with displaced focus  $x_i$  (henceforward designated as the pseudofocus of the lens)

$$\phi_{lens} = \frac{\sum_{i=1}^K W_i \phi_{lens}^{x_i}}{\sum_{i=1}^K W_i} \quad (3)$$

where the Gaussian weight factor reflects the area of the lens that is being illuminated when the feed is at a given position

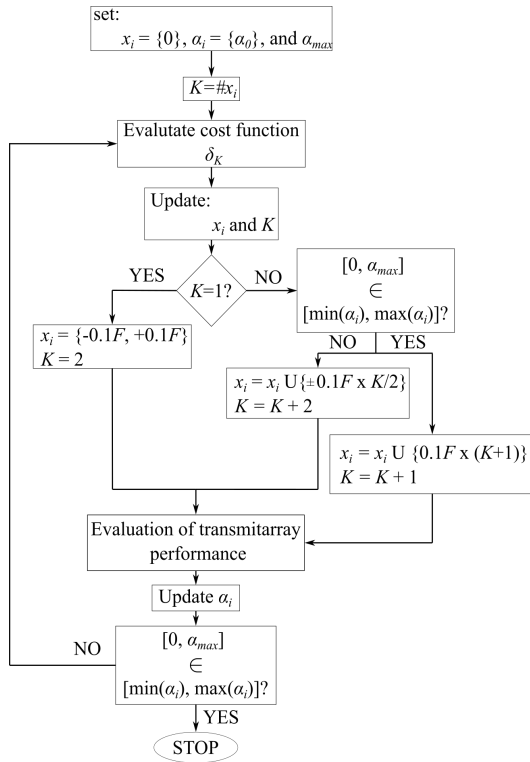


**Figure 3**– Flowchart of the iterative approach used to design the multifocal transmit-array.

$$W_{x_i} = \exp\left(-\frac{(x-x_i)^2 + y^2}{2\sigma^2}\right) \quad (4)$$

The case where  $K = 2$  corresponds to the bifocal design presented in [16]. The standard deviation of the Gaussian illumination  $\sigma$  is directly related to the edge field taper level (in dB),  $\tau_{dB}$

$$\sigma = \frac{D}{\sqrt{\frac{2}{5}\tau_{dB} \ln 10}} \quad (5)$$

The compromise between the aperture efficiency, side lobe level, and spillover results that taper levels,  $\tau_{dB}$ , typically range between 10 and 20 dB. According to (5), for the  $D = 145$  mm aperture dimensions considered herein results that  $\sigma \in [47.8, 33.8]$  mm. A more exact value for this parameter can be retrieved from fitting the Gaussian profile (4) to the primary source radiation pattern.

In (3) it is implicit that the exit angles  $\alpha_i$ , corresponding to each unifocal correction, are known *a priori*. However,  $\alpha_i$  depends on the phase correction of the lens itself, which makes (1) a much more intricate equation that what may seem at first glance. Moreover, it is not known what number of unifocal corrections,  $K$ , should be used in (3). As such, we proposed an iterative approach to tackle this problem, which is depicted in Figure 3 as a flowchart. The inputs of the approach are the set of pseudofocus positions  $x_i$ , their corresponding pointing directions  $\alpha_i$ , and the maximum scanning range  $\alpha_{max}$ . These variables are initialized considering a centered optics transmitarray radiating a beam pointing to  $\alpha_0$ . For every  $(x, y)$  point in the aperture and in each iteration  $K$ ,  $\phi_{lens}^K$  is computed by finding the phase correction that minimizes the following expression considering the set of  $(x_i, \alpha_i)$  pairs obtained in the previous iteration

$$\left(\delta_K = \sum_{i=1}^K W_{x_i} |\phi_{in}^{x_i} + \phi_{lens}^K - g_{ap}^{\alpha_i}|\right)_{min} \quad (6)$$

Then,  $x_i$  is updated according to the paths shown in Figure 3. The perturbation step for the pseudofocus positions is set to  $0.1F$  (being  $F$

**TABLE 1** – Iterative construction of the set  $\alpha_i$  according to the design multifocal design process of Section II.

$x_i/F$	-0.4	-0.3	-0.2	-0.1	0.1	0.2	0.3	0.4	0.5	0.6	0.7
$\alpha_i$	$\alpha_9$	$\alpha_7$	$\alpha_5$	$\alpha_3$	$\alpha_2$	$\alpha_1$	$\alpha_4$	$\alpha_6$	$\alpha_8$	$\alpha_{10}$	$\alpha_{11}$
<b>K=1</b>				37	28						
<b>K=2</b>			42	37	27	23					
<b>K=4</b>		48	42	37	27	23	19				
<b>K=6</b>	53	47	42	37	27	23	19	15			
<b>K=8</b>	53	47	42	37	27	23	19	14	10		
<b>K=10</b>	52	47	42	37	27	22	18	14	9	5	
<b>K=11</b>	52	47	42	37	27	22	18	14	6	2	-3

**TABLE 2** – Iterative GO-PO assessment of the TA performance according to the method described in Section II.

	Min SLL [dB]	Scanning Range [°]	Scan Loss [dB]	Max Dir. [dBi]
<b>K=1</b>	-5.6	46	6.0	32.7
<b>K=4</b>	-7.9	51	4.0	31.9
<b>K=6</b>	-10.0	50	3.6	32.1
<b>K=8</b>	-11.5	51	2.9	31.8
<b>K=9</b>	-11.1	51	2.2	31.3
<b>K=10</b>	-11.1	55	4.3	31.5
<b>K=11</b>	-11.8	51	2.6	31.6

the focal length). For the current  $\phi_{lens}^K$ , the performance of the transmitarray is evaluated for all the pseudofocus positions given by the vector  $\mathbf{x}_K$ . The method for retrieving the radiation pattern of the transmitarray can be GO-PO or full-wave based. From the radiation pattern, the vector  $\alpha_K$  is updated with the new pointing directions. Finally, if the scanning range  $[0, \alpha_{max}]$  is contained in the interval defined by the extremes of the set  $\alpha_K$ , the process stops. Otherwise, the process continues evaluating again (6).

The method relies on the rationale that the phase correction of the transmitarray converges to the natural scanning range promoted by the feed displacement by means of small perturbations. We found that  $0.1F$  is a good perturbation step, however, other values can be considered. It is also important to stress that the cost function (6) does not assume that  $\phi_{lens}^K$  needs to be continuous. Thus, we can adjust this method to any set of unit cells that can only provide a discrete number of phase states. This allows to incorporate in this optimization method the intrinsic discretization error of any set of unit cells. Finally, this method is not limited to GO-PO assessment, although it can be more time-efficient than full-wave based models. Nevertheless, it is also possible to use full-wave analysis to ensure that second order effects, like  $360^\circ$  phase jumps, are accounted for when estimating the beam pointing directions. In our design example we did not find significant advantage in using full-wave analysis instead of faster GO-PO. We only used full wave to validate the performance of the final multifocal TA design. In Figure 2, we compare the radiation patterns obtained by PO-GO simulations following from the multifocal design process (with  $K = 11$ , with the unifocal case ( $\alpha_0 = 32.5, \sigma = 44.8$ ) and aiming at a maximum scanning range of  $\alpha_{max} = 50^\circ$ . Beam steering up to 53 degrees with a SLL below  $-11.8$  dB and 2.6 dB of scan loss is achieved. Given that in the multifocal approach there is never an ideal collimation for any feed position, the maximum gain of this approach (31.6 dBi, in this example) will be always lower than the maximum gain of the unifocal design (32.7 dBi in Figure 2). Nonetheless, the multifocal approach provides a significant improvement on the overall scanning performance of the antenna. This result highlights the tradeoff between the maximum gain and scanning range, which becomes more acute when lower focal distance is considered.

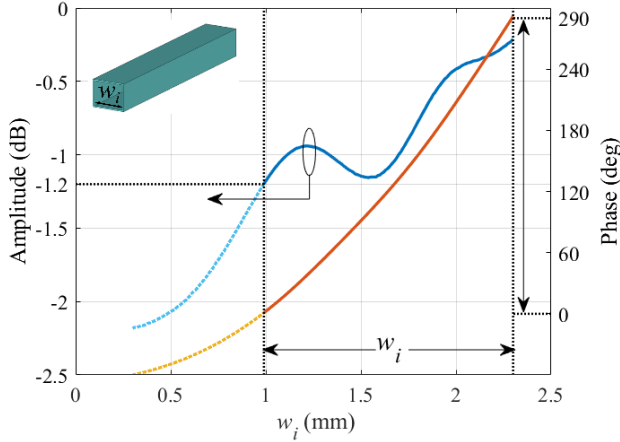


**Figure 4-** Transmission amplitude and phase of the dielectric unit cell.

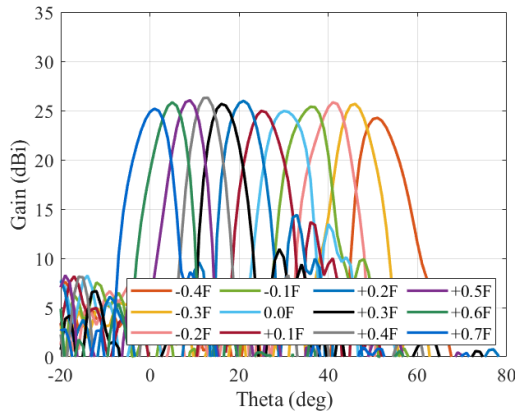


**Figure 5-** Radiation pattern obtained through full-wave simulation of the multi-focal design based on dielectric unit cells at 30 GHz, using a Ka-band open-ended waveguide as feed and a focal distance of 50 mm.

### III. MULTI-FOCAL TRANSMIT-ARRAY USING DIELECTRIC UNIT CELLS

This section summarizes the design of a multifocal TA based on full dielectric unit cells (Figure 4) and a standard WR28 waveguide as the feed of the antenna. The multi-focal TA is designed following the iterative method described in the Section II with the inputs:  $\tau_{dB} = 12$  dB (it corresponds to the illumination at the aperture produced by the open-ended waveguide used as the feed),  $\alpha_0 = 32.5^\circ$  and  $\alpha_{max} = 50^\circ$ . These values are selected to fairly compare the results with other conventional techniques as in [11]. Besides, it should be noted that this geometry reduces by a half of the focal distance (from  $F = 100$  mm to 50 mm) without using a more complex feeding system and the full dielectric unit cells are a broadband solution, so that the bandwidth limitations of this design approach can be also analyzed beyond the frequency limitations associated with resonant unit cells.

Table 1 presents the iterative process for constructing the set of beam pointing directions  $\alpha_i$ . The blank table cells are justified by the iterative process: they are filled progressively at each iteration  $K$ . Table 2 outlines the corresponding main figure of merits obtained during the iterative process. The phase correction of the last iteration ( $K = 11$ ) shows a scanning range up to  $51^\circ$  with a scan loss of 2.6 dB and a maximum directivity of 31.6 dB, preserving the SLL below  $-11.8$  dB.

This phase correction is implemented as a perforated slab of single material block PLA ( $\epsilon_r = 2.98$  and  $\tan \delta = 0.0148$ ), compatible with

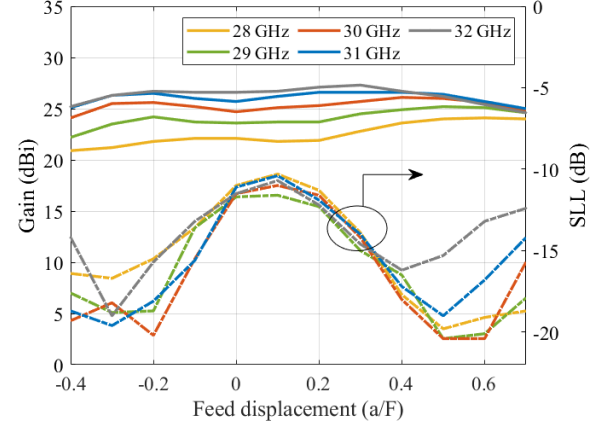


**Figure 6-** Gain and SLL versus the feed displacement obtained through full-wave simulations of the dielectric transmit-array at 30 GHz.

**TABLE 3** – Overall of the in-band response obtained through full-wave simulation for the multifocal TA made up of dielectric unit cells.

Freq. (GHz)	SLL (dB)	$\alpha_{max}$ ( $^\circ$ )	Max Gain (dBi)	$\epsilon_{ap}$ (%)
28	< -10.3	58	24.1	14.22
29	< -11.6	55	25.2	17.08
30	< -11.0	51	26.1	19.63
31	< -10.4	48	26.6	20.63

the most affordable 3D printing solution, FDM. The considered unit cell in-plane dimensions are  $0.25\lambda_0 \times 0.25\lambda_0$  @30 GHz and the cell height is  $1.6\lambda_0$  @30 GHz. The distribution of the perforations follows from unit cell design of TAs. The phase variation of these cells depends on the ratio between air and the dielectric material in the volume that compose the unit cell according to the Maxwell Garnett effective medium theory [21]. The considered air gap volume dimensions are  $w_i \times w_i \times 1.6\lambda_0$  where  $1 \text{ mm} < w_i < 2.3 \text{ mm}$ . The minimum value for  $w_i$  is set by imposing that the transmission coefficients of the unit cells must be above  $-1.2$  dB, necessary due to the high dielectric losses. The criteria of  $-1.2$  dB results from the compromise between transmissivity and phase delay range of the selected set of unit cells. For this criterion, the unit cell phase correction can span continuously a  $290^\circ$  phase interval (Figure 4). On the other hand, the maximum value of  $w_i$  is defined according to the nozzle resolution of the 3D printer. By setting the limit  $w_i = 2.3 \text{ mm}$  the minimum thickness of the dielectric walls of the gaps in the TA is always above 0.2 mm.

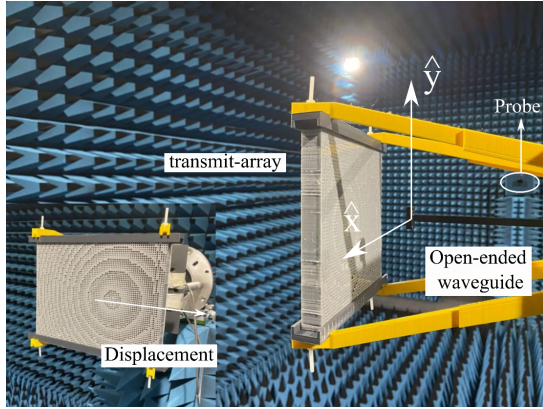
The non-resonant nature of these cells provides a broadband response allowing designing TAs with bandwidths higher than resonant-cell-based designs [22]. The bandwidth performance of the TA antenna is no longer limited by the unit cell response, instead it is limited by the accumulated phase error that arises from the successive 360 phase wraps and unit cell phase quantization. Besides, reducing the total antenna height, TA designs with lower  $F/D$  reduces the gain requirement for the primary feed, which allows using smaller and simpler feeding elements. In this example, we use a standard open-ended waveguide (WR28) as the primary source of the TA which provides an edge taper level close to  $\tau_{dB} = 12$  dB.

The TA phase profile and corresponding unit cell distribution follows from applying the iterative approach described in Figure 3 to the space of solutions for  $\phi_{lens}^K$  provided by the unit cells.

The resulting layout is evaluated in CST Microwave Studio [20], to obtain a full-wave simulation of the design. In Figure 5, the full-wave results are given for the copolar radiation pattern in the azimuth plane at 30 GHz. The maximum gain of the TA is 26.1 dBi while the minima is 24.1 dBi. The scanning stands up to  $50^\circ$  with a scan loss of 2.03 dB.

**TABLE 4** – Comparison between full-wave results and measurements for the different measured positions of the feed at 29, 29.5, and 30 GHz.

			-0.4F	-0.3F	-0.1F	0	+0.1F	+0.3F	+0.5F	+0.7F
29 GHz	Gain (dBi)	Meas.	22.7	23.7	23.7	23.9	22.8	23.3	23.8	23.4
		Sim.	22.2	23.5	23.7	23.6	23.7	24.5	25.2	24.6
	SLL (dB)	Meas.	-18.2	-21.1	-17.5	-16.2	-11.9	-16.4	-17.1	-10.5
		Sim.	-17.6	-18.8	-13.6	-11.7	-11.6	-15.0	-20.4	-17.9
	Pointing dir. (deg)	Meas.	56	50	40	32	27	18	11	3
		Sim.	55	48	38	31	27	16	9	1
29.5 GHz	Gain (dBi)	Meas.	22.7	23.8	23.9	24.3	23.0	24.0	23.8	23.4
		Sim.	23.2	24.7	24.5	24.2	24.4	25.2	25.7	24.7
	SLL (dB)	Meas.	-20.0	-17.8	-18.5	-13.8	-11.9	-16.0	-17.1	-9.5
		Sim.	-19.0	-18.8	-14.7	-11.7	-11.3	-14.4	-20.1	-16.7
	Pointing dir. (deg)	Meas.	55	49	39	32	26	17	10	3
		Sim.	52	47	37	31	25	16	9	1
30 GHz	Gain (dBi)	Meas.	23.4	24.7	24.8	24.9	23.6	24.2	24.2	23.4
		Sim.	24.1	25.5	25.2	24.7	25.1	25.7	26.0	24.8
	SLL (dB)	Meas.	-18.6	-17.8	-19.9	-12.1	-11.4	-15.3	-19.0	-9.0
		Sim.	-19.3	-18.2	-15.5	-11.5	-11.0	-14.2	-20.4	-15.7
	Pointing dir. (deg)	Meas.	53	47	38	31	26	17	10.5	3
		Sim.	51	46	36	30	25	16	9	1

**Figure 7**– TA assembled with the open-ended waveguide in the anechoic chamber.

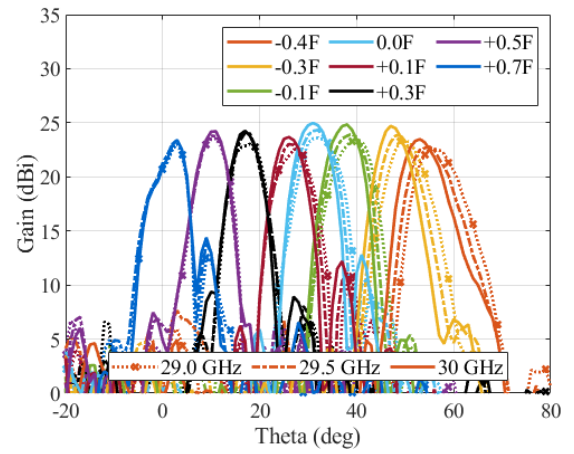
Moreover, the SLL is better than  $-11$  dB (which is the worst case). The high dielectric losses of the PLA results in a radiation of efficiency of  $-0.8$  dB, which could be more significant if the aforementioned  $-1.2$  dB transmissivity criteria were not used for the unit cells. Despite the intrinsic limitation of these dielectric-only unit cells, including a worse angular stability than printed elements, the multifocal approach delivers quite equivalent performance.

Table 3 and Figure 6 outline the in-band analysis of the multifocal transmitarray from 28 GHz to 32 GHz. The antenna presents a similar behavior through the whole band. The scan loss is 3 dB in the worst case (28 GHz), and 1.6 dB at 31 GHz. The SLL is below  $-10$  dB in all the cases and the scan range goes up to  $50^\circ$ . Within the band of interest (29-30 GHz) the beam squint does not have an important impact, obtaining similar outgoing beams. The aperture efficiency ( $\epsilon_{ap}$ ) is nearly 20% at the design frequency, which is expected value in wide angle scanning antennas.

#### IV. EXPERIMENTAL VALIDATION

##### A. Transmit-array manufacture

The multifocal TA developed in the Section III was manufactured. The antenna is printed in the 3D printer Ultimaker 3 using the well-known technique FDM. This technique deposits a thermoplastic material (in this case PLA) through a mobile extruder, printing the prototype layer-by-layer. Figure 7 shows the 3D printed setup used to hold the feed (open-ended Ka-band waveguide WR28) and the TA. This structure enables a physical displacement of the TA, so that an in-plane movement of the feed can be replicated. As shown in Figure 7, the electrical field of the waveguide is y-polarized and the

**Figure 8**– Measured radiation pattern for the scanning cut ( $\phi = 0^\circ$ ) at 29, 29.5, and 30 GHz.

displacement of the transmitarray is made along the  $x$ -axis. The distance between the aperture of the waveguide and the transmitarray antenna was first set to  $F = 50$  mm according to simulations. However, in the measurements, different positions were also tested to find the maximum gain for the centered position of the feed ( $x_i = 0.0F$ ).

For  $F = 47.5$  mm, the TA is evaluated in the anechoic chamber of the University of Oviedo. The setup consists of the TA antenna (AUT), and a Ka-band standard pyramidal horn antenna of 20 dBi used as probe. Both AUT and probe are connected to the ports of a PNA Network Analyzer. The radiation pattern is measured in the spherical range at 29 GHz, 29.5 GHz, and 30 GHz, which covers the uplink of Ka-band satellite systems. The transmitarray is moved according to the  $x$ -axis, emulating 8 different positions of the feed ranging from  $x_i = -0.4F$  to  $0.7F$ . The gain is calculated through the comparison with a calibrated antenna used as reference. According to the datasheet, there is an uncertainty of  $\pm 0.25$  dB in its gain. Thus, to compute the gain of the transmitarray the mean value is used.

##### B. Measurements

The copolar radiation pattern of the TA at the design frequency (30 GHz), and two other additional frequencies (29 and 29.5 GHz) are shown in Figure 8. The radiation pattern is shown for 8 positions to evaluate the scanning performance of the antenna. At the design frequency, the central position of the feed ( $0.0F$ ) presents the maximum gain (24.96 dBi) while the extreme positions ( $-0.4F$  and  $+0.7F$ ) show the lower gain (23.4 dBi). For these positions, the beam

pointing is  $53^\circ$  and  $3^\circ$ . Hence, the resulting scan loss is around 1.5 dB within a scanning range of  $50^\circ$ . Table 4 outlines a comparison between the measurements and full-wave simulations for the three frequencies. As expected from full-wave results, the central beams  $0.0F$  and  $+0.1F$  and the extreme beam  $+0.7F$  show the highest SLL. For those central positions the SLL are lower than  $-11$  dB, while it increases up to  $-9$  dB in the extreme position. The design technique degrades the response of the central beams to enhance the performance within the scanning range.

The copolar radiation patterns at 29 and 29.5 GHz present a similar performance in terms of gain, scanning range and SLL. The maximum gain is obtained at  $0.0F$  in both frequencies, whose maximum is 24.32 dBi (29.5 GHz) and 23.91 dBi (29 GHz). This slight drop in the gain is related to a smaller electrical size of the aperture. The minimal gain is 22.78 dBi and 22.7 dBi in both cases for the feed placed at  $-0.4F$ . A quite stable response of the gain is obtained within the whole scanning range. For the lower frequency, 29 GHz, the scan loss is 1.1 dB within a range of  $53^\circ$ , while at 29.5 GHz the scan loss is 1.5 dB in a range of  $52^\circ$ . The SLL are like the ones obtained at 30 GHz, being the worst case  $-9.59$  dB (29.5 GHz) and  $-10.51$  dB (29 GHz), when the feed is at  $0.7F$ . Besides, the SLL at  $0.1F$  is  $-11.90$  dB at both frequencies and like 30 GHz.

The overall performance of the beams presents a similar behavior through the whole scanning range and the three frequencies. Besides, the agreement between full-wave results and the measurements is good. The slight difference might be associated to different factors. The presented prototype is manufactured with FDM. This is a very affordable technique at the cost of decreasing the control on the accuracy comparing with other classical techniques. In addition, the incident field provided by the open-ended Ka-band waveguide could be slightly different from the one used in simulations due to the experimental initial adjustment of the feed position. Despite these factors the measurements strongly agree with full-wave results at the three frequencies. It is worthy to note that the pointing beam direction is well predicted from full-wave simulations and the beam squint has a maximum deviation of  $3^\circ$ . However, for most of the positions of the feed it is nearly  $1^\circ$ .

## V. CONCLUSION.

A novel technique is presented to design wide-angle mechanical beam scanning TAs to obtain high-gain and cost-effective solutions for low-profile terminals. In the design of compact terminals ( $F/D < 0.5$ ), the scanning aberrations produced by the mechanical displacement of the feed is an important limiting factor. The proposed technique allows overcoming these limitations by using an iterative method to obtain a phase correction on the TA that evenly distributes the scanning aberration among all the outgoing beams. The design carried out with this technique shows excellent performance within a wide scanning range of  $50^\circ$  and low scan loss from 29 to 30 GHz. The proposed technique notably improves the scanning performance compared to conventional single-focus phase corrections, especially for low  $F/D$  ratios. Moreover, this method is general, it can be extended to reflective surfaces, both metasurface and reflectarray antennas, irrespective of the unit-cell technology.

## REFERENCES

- [1] J. Wen, C. Wang, W. Hong, Y. Pan, and S. Zheng, "A wideband switched-beam antenna array fed by compact single-layer butler matrix," *IEEE Trans. Antennas Propag.*, vol. 69, no. 8, pp. 5130-5135.
- [2] G. Wu, S. Qu, S. Yang, and C. Chan, "Low-cost 1-D beam-steering reflectarray with  $\pm 70^\circ$  scan coverage," *IEEE Trans. Antennas Propag.*, vol. 68, no. 6, pp. 5009-5014, Jun. 2020.
- [3] M. Wang, S. Xu, N. Hu, W. Xie, F. Yang, and Z. Chen, "A low-profile wide-angle reconfigurable transmitarray antenna using phase transforming lens with virtual focal source," *IEEE Trans. Antennas Propag.*, Early Access.
- [4] R. Lo Forti, G. Bellaveglia, A. Colasante, E. Shabirow, and M. Greenspan, "Mobile communications: High-speed train antennas from Ku to Ka," in *Proc. 5th Eur. Conf. Antennas Propag. (EuCAP)*, Rome, Italy, Apr. 2011, pp. 2354-2357.
- [5] P. Nayeri, F. Yang, and A. Z. Elsherbeni, "Bifocal design and aperture phase optimizations of reflectarray antennas for wide-angle beam scanning performance," *IEEE Trans. Antennas Propag.*, vol. 61, no. 9, pp. 4588-4597, 2013.
- [6] G. Wu, S. Qu, and S. Yang, "Wide-angle beam-scanning reflectarray with mechanical steering," *IEEE Trans. Antennas Propag.*, vol. 66, no. 1, pp. 172-181, Jan., 2018.
- [7] Y. J. Guo, M. Ansari, R. W. Ziolkowski, and N. J. G. Fonseca, "Quasi-optical multi-beam antenna technologies for B5G and 6G mmWave and THz networks: A Review," *IEEE Open Journal of Antennas and Propagation*, vol. 2, pp. 807-830, 2021.
- [8] C. Wang, Y. Xia, G. Guo, M. Nasir, and Q. Zhu, "Ellipsoidal Luneburg lens binary array for wide-angle scanning," *IEEE Trans. Antennas Propag.* Vol. 68, no. 7, pp. 5702-5707, Jul. 2020.
- [9] N. J. Fonseca, Q. Liao, and O. Quevedo-Teruel, "Compact parallel-plate waveguide half-Luneburg geodesic lens in the Ka-band," *IET Microw. Antennas Propag.*, 15:123-130.
- [10] S. A. Matos, E. B. Lima, J. S. Silva, J. R. Costa, C. A. Fernandes, N. J. G. Fonseca, J. R. Mosig, "High gain dual-band beam-steering transmit array for Satcom terminals at Ka-Band," *IEEE Trans. Antennas Propag.*, vol. 65, no. 7, pp. 3528-3539, July 2017.
- [11] E. B. Lima, S. A. Matos, J. R. Costa, C. A. Fernandes, and N. J. G. Fonseca, "Circular polarization wide-angle beam steering at Ka-band by in-plane translation of a plate lens antenna," *IEEE Trans. Antennas Propag.*, vol. 63, no. 12, pp. 5443-5455, Dec. 2015.
- [12] Cornbleet, Sidney. "Microwave and geometrical optics." *Techniques of physics* (1994).
- [13] J. Rao, "Multifocal three-dimensional bootlace lenses," *IEEE Trans. Antennas Propag.*, vol. 30, no. 6, pp. 1050-1056, Nov. 1982.
- [14] W. Rotman and R. Turner, "Wide-angle microwave lens for line source applications," *IEEE Trans. Antennas Propag.*, vol. 11, no. 6, pp. 623-632, Nov. 1963.
- [15] E. Martinez-de-Rioja et al., "Bifocal technique applied to dual transmitarray antennas," in *12th European Conference on Antennas and Propagation (EuCAP)*, 2018, pp. 1-5, doi: 10.1049/cp.2018.0869.
- [16] S. A. Matos, E. B. Lima, J. R. Costa, C. A. Fernandes and N. J. G. Fonseca, "Design of a 40 dBi planar bifocal lens for mechanical beam steering at Ka-band," in *2016 10th European Conference on Antennas and Propagation (EuCAP)*, 2016, pp. 1-4.
- [17] Wang, H.-f., Wang, P.-c., Wang, Z.-b., Zhang, H.-m. and Zhang, Y.-r. (2020), Beam scanning antenna based on parabolic phase distribution lenses. *IET Microw. Antennas Propag.*, 14: 505-509.
- [18] P. Nayeri, F. Yang and A. Z. Elsherbeni, "Design of multifocal transmitarray antennas for beamforming applications," in *2013 IEEE Antennas and Propagation Society International Symposium (APSURSI)*, 2013, pp. 1672-1673.
- [19] J. M. Felício et al., "Complex permittivity and anisotropy measurement of 3D-printed PLA at microwaves and millimeter-waves", in *22nd Int. Conf. on Applied Electromagnetics and Communications (ICECOM)*, Dubrovnik, Croatia, 2016.
- [20] Systèmes, Dassault. "CST microwave studio." computer program] Available at: <http://www.cst.com> [Accessed: 11 January 2022] (2021).
- [21] A. H. Sihvola and J. A. Kong, "Effective permittivity of dielectric mixtures," *IEEE Trans. Geoscience and Remote Sensing*, vol. 26, no. 4, pp. 420-429, July 1988.
- [22] S. A. Matos et al., "3-D-Printed transmit-array antenna for broadband backhaul 5G links at V-band," *IEEE Antennas and Wireless Propagation Letters*, vol. 19, no. 6, pp. 977-981, June 2020.